

Livelayer: A Semi-Automatic Software for Segmentation of Layers and Objects in Optical Coherence Tomography Images

Mansooreh Montazerin, Zahra Sajjadifar, Rahele Kafieh

Abstract:

The Ophthalmology Science has recently witnessed marked progress due to the advent of divergent imaging techniques, especially Optical Coherence Tomography (OCT) which has caught many physicians' attention for being exact, rapid, non-invasive and low-cost. Given these interesting features of OCTs as well as the capacity to display symptoms of a wide variety of eye diseases and neurological disorders, the need for OCT image segmentation and the corresponding data interpretation is felt more than ever before. In this paper, we wish to address this need and solve the difficulties associated with OCT image segmentation by offering a handy software written in the MATLAB App Designer environment which helps researchers and clinicians to easily segment the images, save the numerical outcomes and send them for proper analysis. Serving an unambiguous user interface along with a unified platform in which all necessary functions have been incorporated graphically has made this software so unique that it could be recommended to anyone tending to work on ocular OCT layers and fluid segmentation. The software also accommodates a novel graph-based semi-automatic method, called Livelayer and designed for straightforward segmentation of retinal layers and fluids.

Keywords:

Optical Coherence Tomography; Semi-Automatic Layer Segmentation; Ocular Images; Fluid Segmentation

Code metadata description:

1. Motivation and Significance

Optical Coherence Tomography (OCT) is a non-invasive, relatively inexpensive imaging technique based on low-coherence interferometry and captures high-resolution multi-dimensional images from biological tissue especially the retina [1]. Macular OCT images are widely used to assist ophthalmologists in diagnosing ocular deformities such as Diabetic Macular Edema (DME), Glaucoma, Retinal Detachment and Macular Degenerations [2]. In addition to that, their interesting application in diagnosis and effective treatment of some neurodegenerative diseases like Multiple Sclerosis (MS) and Neuromyelitis Optica (NMO) has attracted a lot of neurologists all over the world since these abnormalities have recently turned out to show their early signs in multiple parts of the eye's tissue and therefore, in OCTs [3].

Retina is generally formed by a number of different layers each with a particular shape and thickness. These layers typically lose their standard features with the occurrence of different diseases and measuring the quantitative amount of their structural conversion, provides instructive information about the type, severity and the must-be-employed treatment procedure of that disease [4]. Furthermore, the eye is filled with intraocular fluid which maintains sufficient pressure in the eyeball and is divided into two main portions: aqueous and vitreous humor. When the intraocular fluid changes its position and is leaked into the macula by abnormal blood vessels other kinds of diseases may be caused and fluids may be revealed in OCT images [5].

Regarding the retina anatomy, depicted by OCT, a 3 dimensional OCT from macula is made from successive B-Scans which are two-dimensional cross-sectional views of the central portion of the retina (macula). Besides, a 2 dimensional peripapillary OCT data may be taken from the area surrounding the bundle of nerve fibers at the back of the eye, called optic nerve head (ONH). In order to provide a software for segmentation of inter-retinal layers and fluids in each B-Scan, assorted manual, semi-automatic and full-automatic approaches have been suggested. Whereas, the manual segmentation is both time-consuming and exposed to probable errors, automatic and semi-automatic algorithms have been introduced to solve these problems and are proved to satisfy most physicians (and computer users) who are in charge of OCT segmentation. Since rarely are full-automatic methods capable of being nicely applied to all sorts of OCT images, the semi-automatic segmentation concept has been offered to not only address this issue, but also to supply the Gold Standard data for the full-automatic method's testing and training stage. An abstract table containing a list of previous works on semi-automatic OCT segmentation is presented in Table 1. However, such algorithms suffer from noticeable constraints because they mostly support only one data format, do not suggest various segmentation methods to the users, do not perform a detailed process on the input data like denoising or filtering and finally, they are not integrated in an open-source, user-friendly software environment to make doctors contented by easing the segmentation proceedings for them.

In this paper, we wish to solve the difficulties associated with OCT image segmentation by offering a handy software written in the MATLAB [6] App Designer environment which helps researchers and clinicians to easily segment the images, save the numerical outcomes and send them for proper analysis. Our proposed software consists of independent tabs each responsible for a special function and capable of being used by either professionals or amateurs. In the "File" tab, the user could open his desired data format and convert it to an exclusive format compatible with any other MATLAB code substituted with ours and put aside OCT data format converter software. The next three tabs are

assigned for layer and fluid segmentation of macular B-Scans. The “Manual Layer Segmentation” tab asks the user to input completely manual segmentation of retinal layers and could be used for construction of Gold Standards and error calculation. This block saves useful information about segmented layers in a MATLAB “.mat” file in a folder with a predetermined name. Meanwhile, we have designed the “Auto Layer Segmentation” tab to take the responsibility of the software’s main algorithm, a graph-based semi-automatic segmentation, termed Livelayer, and to obtain each boundary in the order that we have defined. It also has an option for semi-automatic layer correction on the assumption that a faulty boundary should be reformed. Fluids’ identification and localization is the “Fluid Segmentation” tab’s duty which adopts both manual and semi-automatic techniques and maintains all its classified information in a MATLAB structure. Lastly, there is a block for vascular, arcuate peripapillary images to be pre-processed, denoised and segmented in the fifth tab named the “Peripapillary” tab.

Table 1. Description of preceding algorithms for OCT semi-automatic layer and fluid segmentation

Algorithm’s Name	Input	Number of Detected Layers	Location of Segmentation
EdgeSelect [7] (2013)	SD-OCT (Heidelberg Spectralis)	3 Retinal Layers/4 Boundaries (ILM,IS/OS,RPE,BM)*	Macula
Kago-Eye2 [8] (2018)	SD-OCT	2 Borders (C-S,S-H)	Choroid
Zhao’s Method [9] (2012)	SD-OCT	9 Retinal Layers (ILM, NFL/GCL, IPL/INL, INL/OPL, OPL/ONL, ELM, IS/OS, OS/RPE, RPE/CH)*	Macula
Liu’s Method [10] (2018)	Duke Diabetic Macular Edema & POne datasets	8 Categories (ILM, NFL-IPL, INL, OPL, ONL-ISM, ISE, OSE-RPE, Fluids)*	Macula
SAMIRIX [11] (2019)	Spectralis SD-OCT & Heidelberg Eye Explorer (HEYEX) (.vol format)	9 Boundaries (ILM, RNFL-GCL, IPL-INL, INL-OPL, OPL-ONL, ELM, IS/OS, OPT- RPE, BM)*	Macula

Each retinal layer’s abbreviation stands for as follows: ILM: Inner Limiting membrane, NFL: Nerve Fiber Layer, GCL: Ganglion Cell Layer, IPL: Inner Plexiform Layer, INL: Inner Nuclear Layer, OPL: Outer Plexiform Layer, ONL: Outer Nuclear Layer, ELM: External Limiting Membrane, IS/OS: Inner and Outer Segment, RPE: Retinal Pigment Epithelium, BM: Bruch’s Membrane, CH: Choroid.

2. Software Description

The software comprises 5 main tabs, namely File, Manual Layer Segmentation, Auto Layer Segmentation, Fluid Segmentation and Peripapillary, each of which has its own specific function. In addition to being able to work with different OCT data formats, with the aid of our designed software, the user would reap the benefits of various segmentation methods for OCTs and fluids, a decent layer

correction procedure, a precise and suitable algorithm for peripapillary segmentation and ultimately, a saving functionality which is considered to be the most important part of the software and stores all relevant coordinates, masks and images in a classified manner.

2.1. File Tab

OCT images can be of various formats. We've put three formats that are most commonly used so that the user can select the desired one and load it into the MATLAB software environment. In this section, after loading data with one of the ".mat", ".octbin" or ".bin" formats, the user has an overview of different B-Scans using the top spinner assuming that the loaded file has multiple B-Scans. The rotate button is set to rotate the image by 90, 180 or 270 degrees. Additionally, there is a text box in which the user types an appropriate path ending with a specific file name (e.g. the name of the patient) to save all layers and fluids' coordinates and information (Fig. 1).

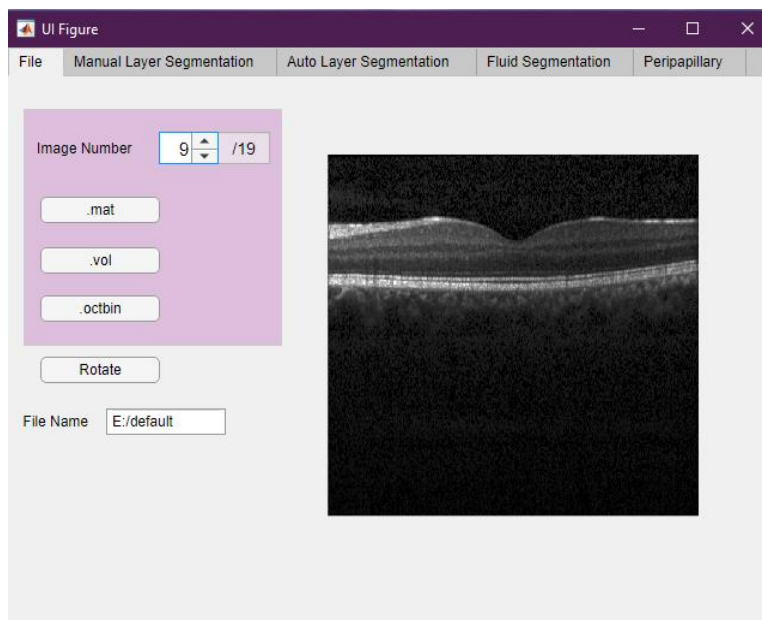


Fig. 1. Demonstration of the File tab.

2.2. Manual Layer Segmentation Tab

If the user wishes to entirely acquire a boundary manually, he should make use of this tab which works with MATLAB "imfreehand" function. The user pushes the mouse and drags it over the boundary. Every time his hand is picked up, a question dialogue appears on the figure and asks whether the user wants to continue or not (Fig. 2). As long as the answer is yes, multiple parts of the boundary are

obtained and once the answer turns to no, these parts are joined together and smoothed to make an entity for each selected boundary (Fig. 3).



Fig. 2. Manual segmentation with “imfreehand” function.

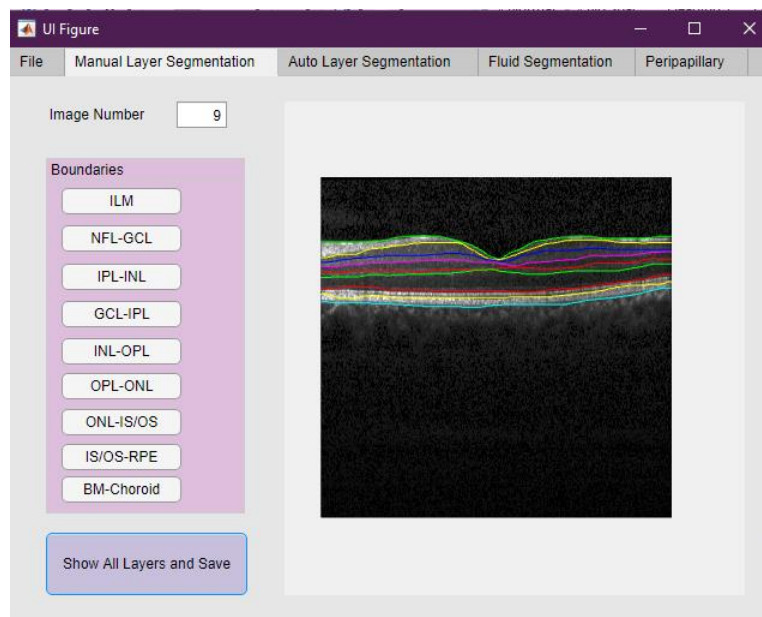


Fig. 3. Manual Layer Segmentation tab.

2.3. Auto Layer Segmentation Tab

This block displays two possibilities for semi-automatic segmentation of retinal layers and only a few clicks are needed, compared to the “Manual Layer Segmentation Tab”.

2.3.1. Semi-Automatic Tab using the Livelay method

In this tab, the user chooses his desired B-Scan as well as the boundary to-be-detected on the left hand side of the app window. Then, a MATLAB figure opens up waiting for a click on the first pixel of the opted boundary to call the Dijkstra algorithm [12]. The Dijkstra algorithm finds the shortest path between a pair of nodes (pixels) in a graph (that is made from the image). We have used its interactive variant, called the

livewire technique [13], in which, the original image is accepted for construction of the graph. After clicking on the initial pixel of the desired path, as the user moves the mouse along the path, the livewire displays the smallest cost path based on the brightness of pixels in the original image. He should drag the mouse on the path so as to discover a route which best fits that path and pause the livewire by clicking on, whenever he observes that the route has become inappropriate. He then, resumes by clicking on the previous pixel beside the last one and this process proceeds until the entire path is acquired (Fig. 4). The user should press the enter key at this time to stop running the livewire and to close the figure.

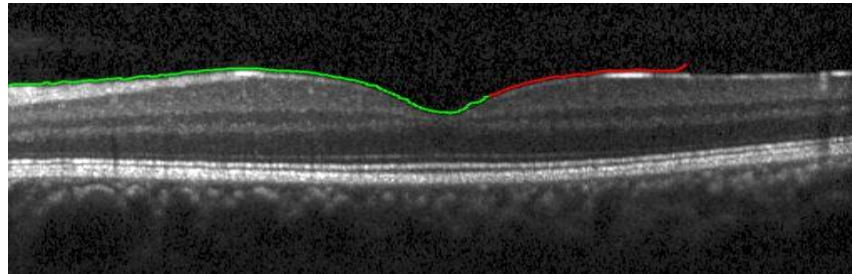


Fig. 4. Semi-automatic segmentation with “Livewire” function

The conventional Livewire, applied over the original image, is not capable of following the OCT boundaries due to their weak and vague appearance in B-Scans and the intended boundary needs to be completely isolated before being fed into the livewire. Therefore, our proposed Livelayer method is created on the basis of the original livewire and is applied to different processed versions of the original image which have the ability to sharpen the desired boundary. Accordingly, we select an image, in which, the outline of that boundary is sufficiently discernible so that it can be captured by the Livelayer function with the least number of clicks. We detect these best sharpened boundaries by utilizing diverse methods of edge detection [14],[15],[16],[17],[18]. Similar to Livelayer, the proposed semi-automatic method can also be applied over B-Scans containing fluid objects, by providing sharpened edges for the fluids. A brief illustration of conducted operations on the original OCT image, leading to an apt background image for segmentation is shown in Fig. 5 and Fig. 6.

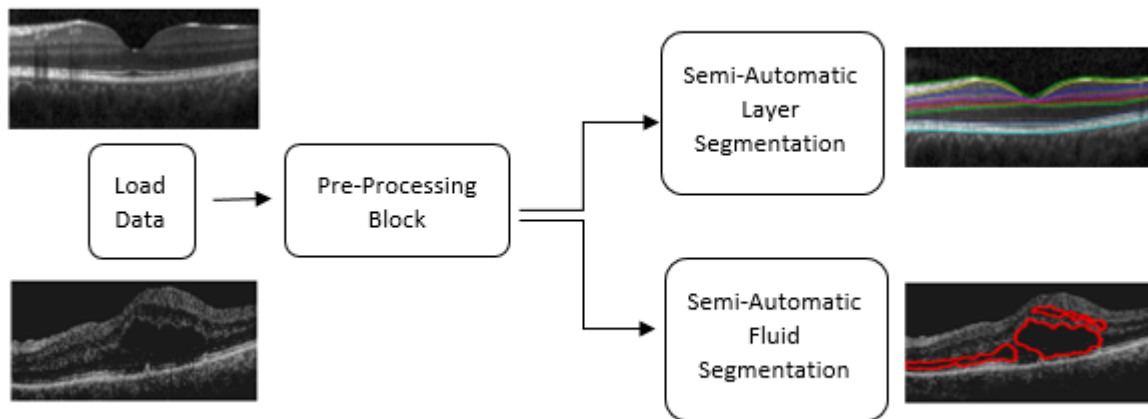


Fig. 5. An overview of operations done for production of an apt background image for segmentation

As can be seen in Fig. 6, fluid segmentation and Livelayer in 8 out of 9 boundaries require a preprocessing step with edge detection and morphological operations to achieve the best graph weights for Dijkstra algorithm.

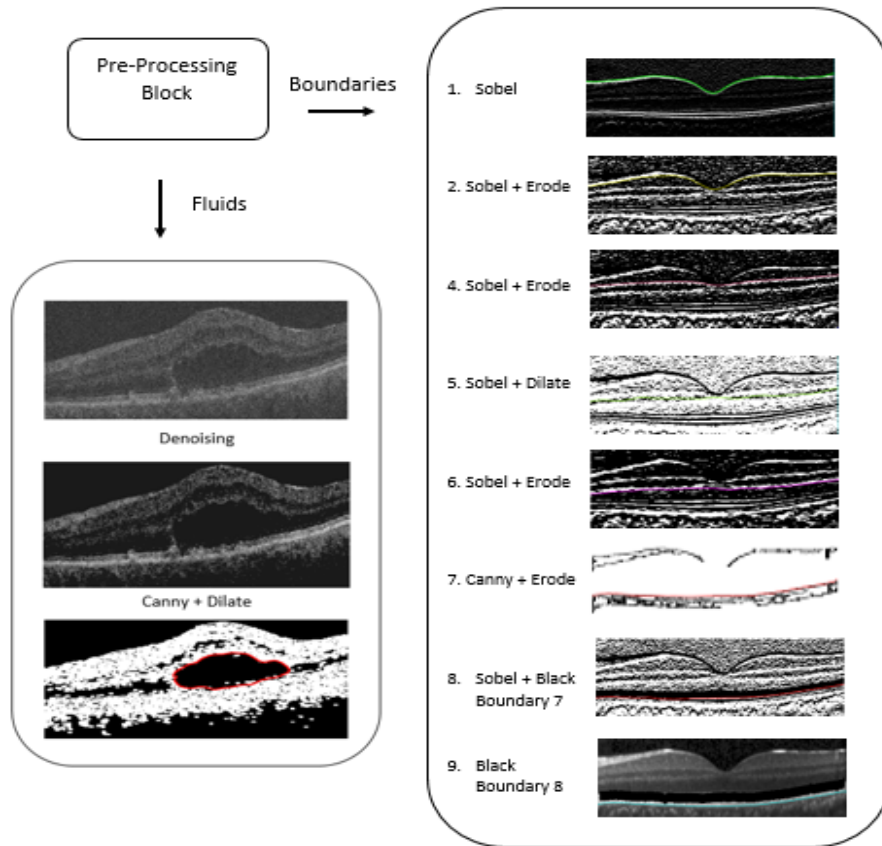


Fig. 6. Illustration of the pre-processing block in Fig. 5

However, it is evident from Fig. 6 that the third boundary (located between GCL and IPL) is not listed for the semi-automatic Livelayer and cannot be obtained by our suggested method since it is not clearly found in the macula's B-Scans. Thus, the user should acquire the fourth boundary immediately after the second, while the third boundary is found automatically by locations of the minimum brightness between boundaries 2 and 4 in the Y-Gradient of the main image being attributed to it. Therefore, it is of vital importance that the user follows a specific sequence in acquiring the boundaries. To facilitate moving between boundaries by the user, we have made colored lamps demonstrating the state of each boundary. Whereas the green color indicates that the boundary is acquired completely, yellow and red colors are signs of partially and not acquired boundaries, respectively. Finally, the attained boundaries are passed through a smoothing stage and are plotted on each B-Scan while the corresponding Y coordinates are saved in a ".mat" file (Fig. 7). Notice that the number of clicks (in semi-automatic Livelayer) depend both on the image quality and that the intrinsic characteristics of that boundary on the image.

The mean number of clicks during the semi-automatic Livelayer and the required time (in seconds) for each boundary to be entirely acquired is calculated by averaging over 10 images as indicated in Table 2.

Table 2. Number of clicks and required time for the semi-automatic method

	ILM	NFL-GCL	IPL-INL	INL-OPL	OPL-ONL	ONL-IS/OS	IS/OS-RPE	BM-Choroid	Total
Number of Clicks	2.1	3.1	2.5	4.3	4	3.3	2.4	2.7	-
Required Time	3.58	5.64	6.14	8.92	5.98	6.34	7.62	4.47	48.69

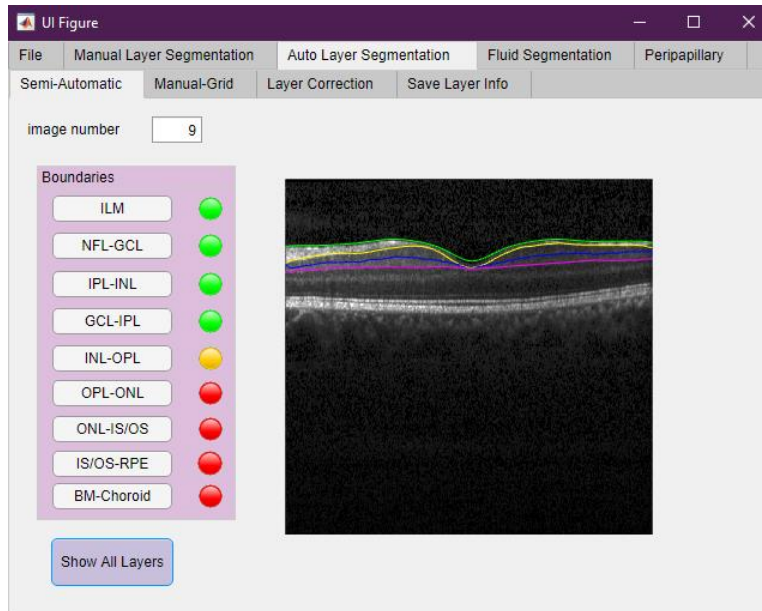


Fig. 7. Semi-Automatic tab of the Auto Layer Segmentation tab.

2.3.2. Manual-Grid Tab

Unlike the Manual Layer Segmentation Tab in 2.2, this tab does not need continuous entry of boundary points by the user. Instead, the user chooses the to-be-segmented boundary and enters the number of adequate vertical lines by which that boundary should be gridded. After that, a gridded B-Scan opens up in a figure in order for the user to click the boundary exactly on the plotted vertical lines (on a limited number of points) (Fig. 8). When finished, the interpolated boundary is depicted on the B-Scan and its Y coordinates are saved in a “.mat” file (Fig .9).

Table 3 represents the calculated time (in seconds) for obtaining a boundary that is equally divided into 10 portions and has no integral distortion (if distortion increases, number of lines would reach maximum of 15 for our tested images):

Table 3. Required time for the manual-grid method

	ILM	NFL-GCL	GCL-IPL	IPL-INL	INL-OPL	OPL-ONL	ONL-IS/OS	IS/OS-RPE	BM-Choroid	Total
Required Time	23	22	22	21	20	21.5	20.25	20.2	16	185.95

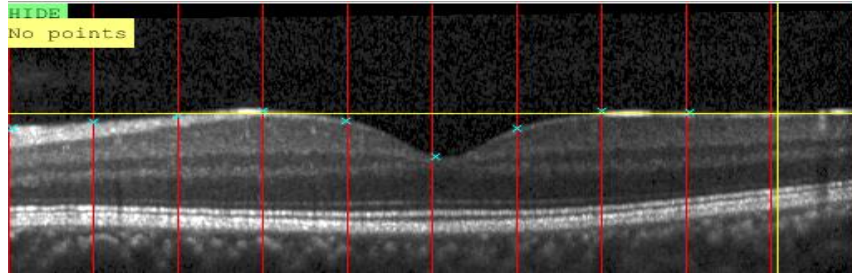


Fig. 8. Clicking on vertical lines in the manual-grid method

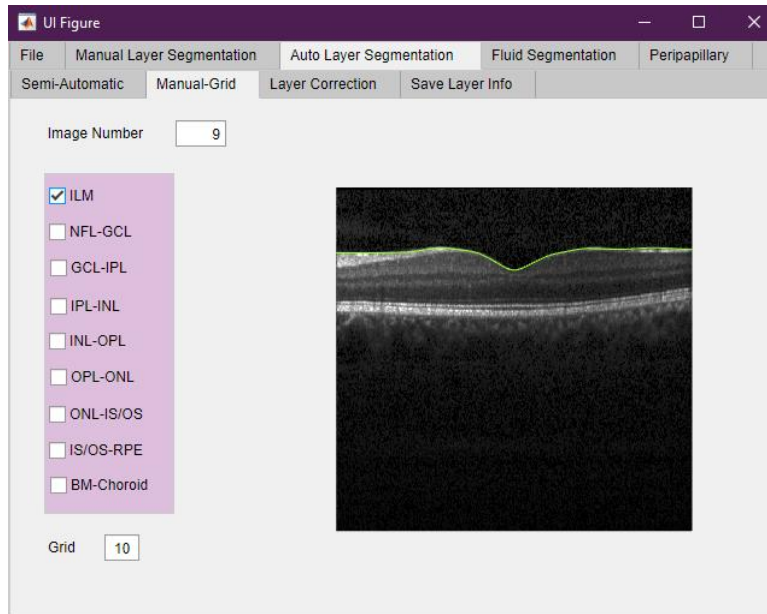


Fig. 9. Manual-Grid tab

2.3.3. Layer Correction Tab

Even after a meticulous segmentation, the final result may not be pretty perfect. So, we have provided a chance for the user to manually correct the defective boundaries. The user should first, click on the beginning and end of the intended path for correction. This path is omitted and gridded by vertical lines the number of which should be set by the “Grid” textbox. The following steps is exactly like the Manual-

Grid layer segmentation explained in 2.3.2 (Fig. 10). When finished, the corrected boundary is replaced with the inaccurate one in the corresponding “.mat” file (Fig. 11).

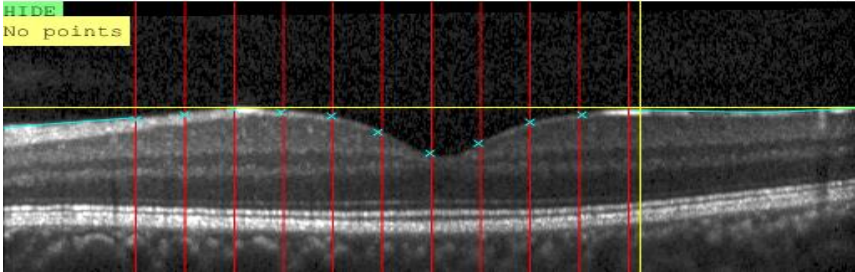


Fig. 10. Layer correction using the manual-grid method

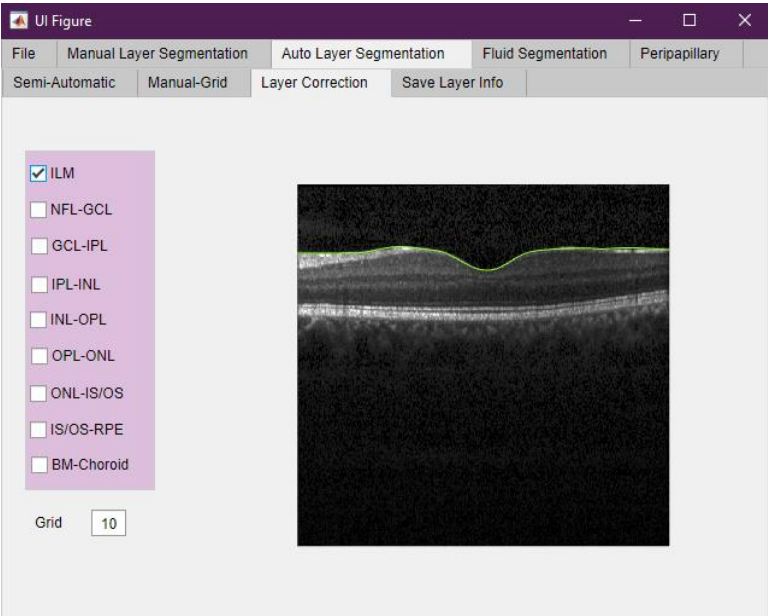


Fig. 11. Layer Correction tab

2.3.4. *Save Layer Info Tab*

“Show All Layers and Save” button in this tab is utilized only if all boundaries are acquired (Fig. 12) and it saves all information related to the app’s semi-automatic section.

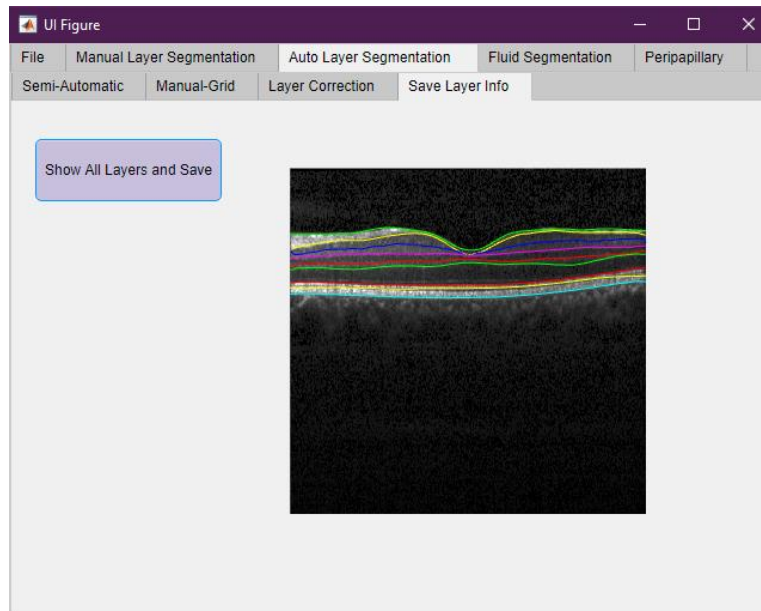


Fig. 12. Save Layer Info tab

2.4. *Fluid Segmentation Tab*

Fluids appear as cysts due to various diseases, including diabetes and hypertension [19]. There are different types of fluids with regard to their position. Intra-Retinal Fluid (IRF) normally appears above Outer Plexiform Layer (OPL), Sub-Retinal Fluid (SRF) is dark accumulations of fluid beneath the Outer Segment Layer (OSL) [20] and Pigment Epithelial Detachments (PEDs) are related to a condition where the Retinal Pigment Epithelium (RPE) detaches from Bruch's Membrane due to the buildup of fluid or blood between these layers [21]. In this section, we have employed two distinct techniques to locate all kinds of fluids (Fig. 13).

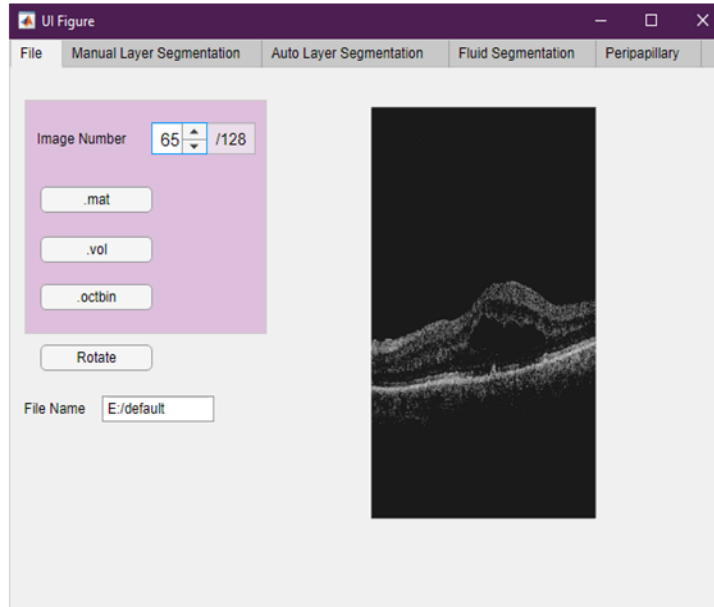


Fig. 13. File tab, appropriate B-Scan selection

2.4.1. Semi-Automatic Tab

The first tab enables the user to segment fluids by a semi-automatic approach using the Livelayer function, process of which is elaborated in the “Semi-Automatic Layer Segmentation” tab. Briefly, the user enters the desired B-Scan number and then, selects the fluid type he would like to find from the three types shown in the left hand side (IRF, SRF, PED). Therefore, the program enters an infinite loop and receives as many objects as the user wants and the text box value indicating the “Number of Objects” is added automatically when each object is taken. If the user finds an object incorrectly and prefers to delete it, he can click on the “Delete” button and obtain the deleted object again. After detecting all planned fluids, by clicking on the “Finish” button, all fluid coordinates and their mask images could be stored in a MATLAB structure (Fig. 14).

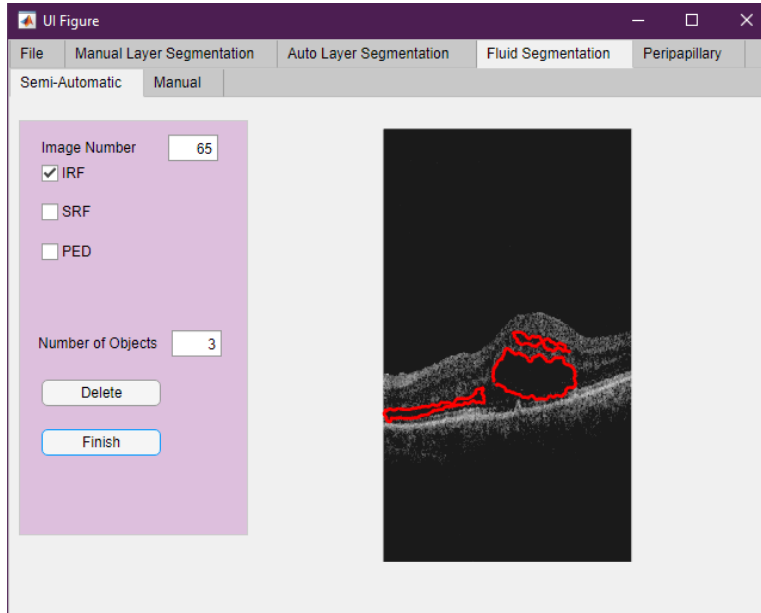


Fig. 14. Semi-Automatic tab of the Fluid Segmentation tab

2.4.2. Manual Tab

The second tab acts exactly like the first tab except that the fluids are found manually using the MATLAB “imfreehand” function. Here, unlike the “Manual Layer Segmentation” tab, there is no question dialogue when user’s hand is picked up. Alternatively, every time the user pushes the mouse and drags it over the fluid’s boundary and picks his hand up, one separate fluid is recognized (Fig. 15).

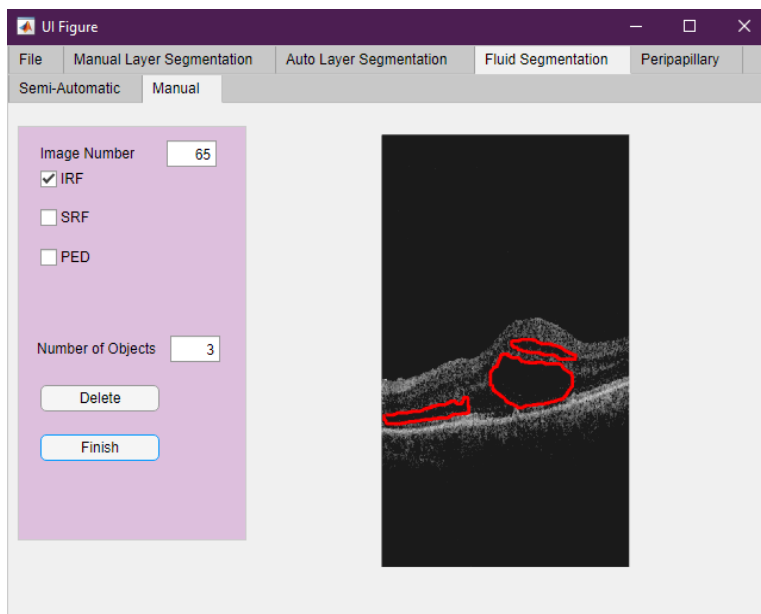


Fig. 15. Manual tab of the Fluid Segmentation tab

2.5. Peripapillary Tab

This tab is allocated to segment layers of peripapillary images using the offered semi-automatic Livelayer. However, in contrast to macular B-Scans, existence of veins and the arcuate structure in these images can disturb the process of livewire function. Hence, pragmatic approaches are adopted for image enhancement before applying the Livelayer. The general procedure of this tab is illustrated in Fig. 16.

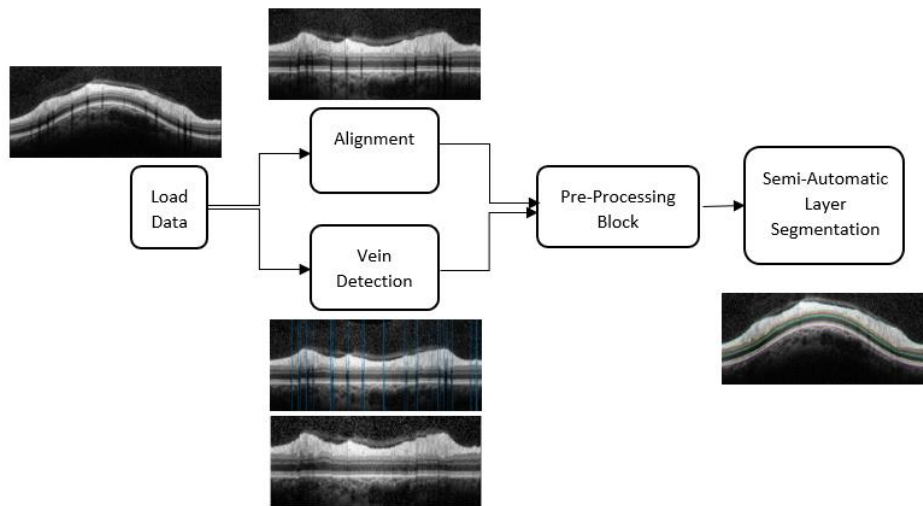


Fig. 16. The block diagram of the Peripapillary tab

2.5.1 Alignment

To align all boundaries, we need to circularly shift each column of the image by its corresponding value in a shift vector which is produced by subtracting all Y-coordinates of a reference boundary (e.g. the 6th boundary) from the maximum amount. This vector has the same length as the image's width and its elements show the number of pixels causing the arcuate structure of the reference boundary. By choosing the sixth boundary as a reference and easily obtaining it with the Livelayer function, the shift vector for the MATLAB "circshift" function is determined and subsequently, the arc becomes flattened.

2.5.2 Vein Detection

In order for veins to be omitted, the user must acquire the third boundary on the flattened image to calculate the mean value of every column located between the third boundary to bottom of the image. Since veins appear in black in ocular images, local minima and maxima of these mean values are their exact locations. To find the beginning, the end and consequently the width of the veins, derivative of the mean above-suggested vector is computed and by employing "islocalmin" and "islocalmax" MATLAB functions, relative extrema are figured out while one of which (minima), introduces the beginning and the other (maxima), offers the end of the veins' locations (Fig. 17). It is apparent that the width of the veins is achieved by subtracting the minima from maxima. Finally, the

right (left) half of the vein is replaced by adjacent right (left) columns, therefore the veins are quite eliminated and the peripapillary image is prepared to be segmented.

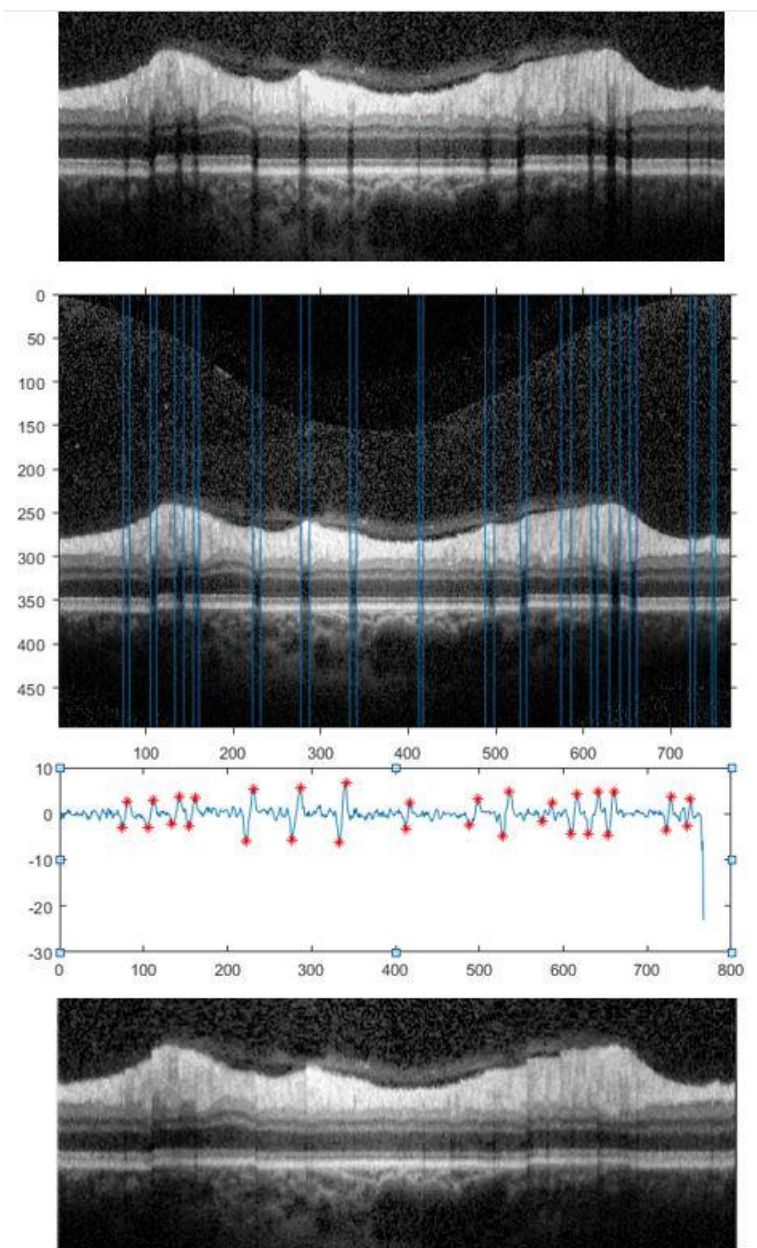


Fig. 17. Relative extrema's (veins') location figured out through mean vector derivation

2.5.1 Pre-Processing Block

Similar to the macula's semi-automatic method, for each boundary in peripapillary OCTs, we need to adopt edge sharpening measures before using Livelayer. We mostly apply gradient and canny functions over peripapillary images (detailed steps are demonstrated in Fig. 18 and 19).

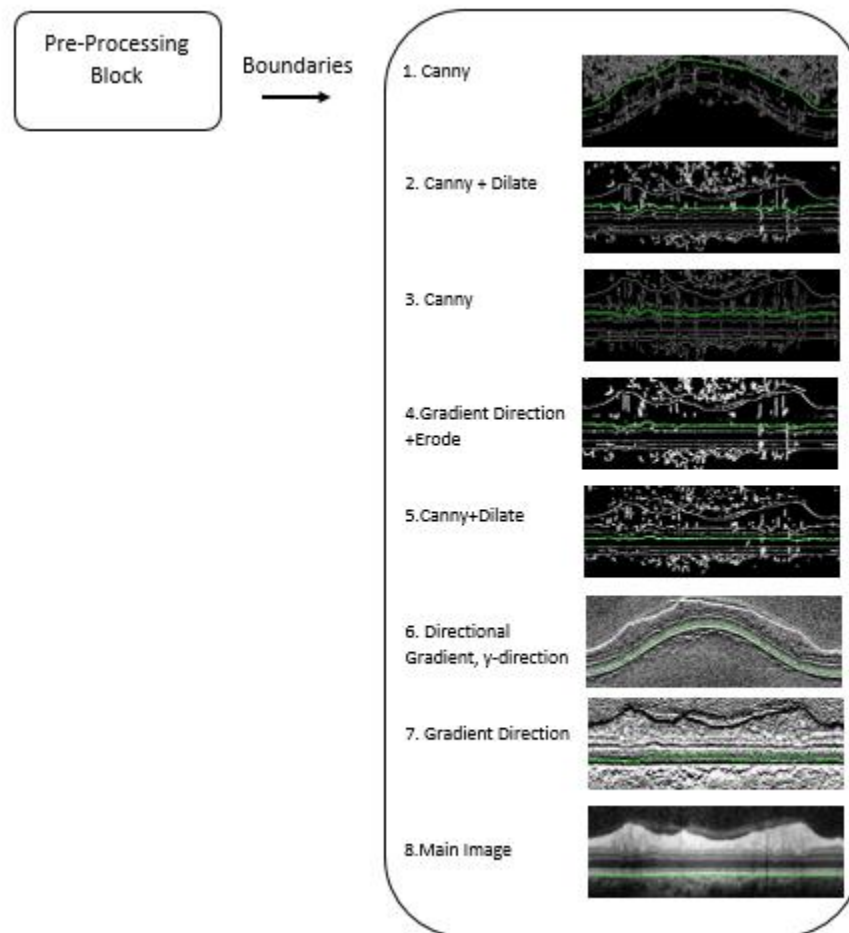


Fig. 18. Illustration of the pre-processing block in Fig. 16

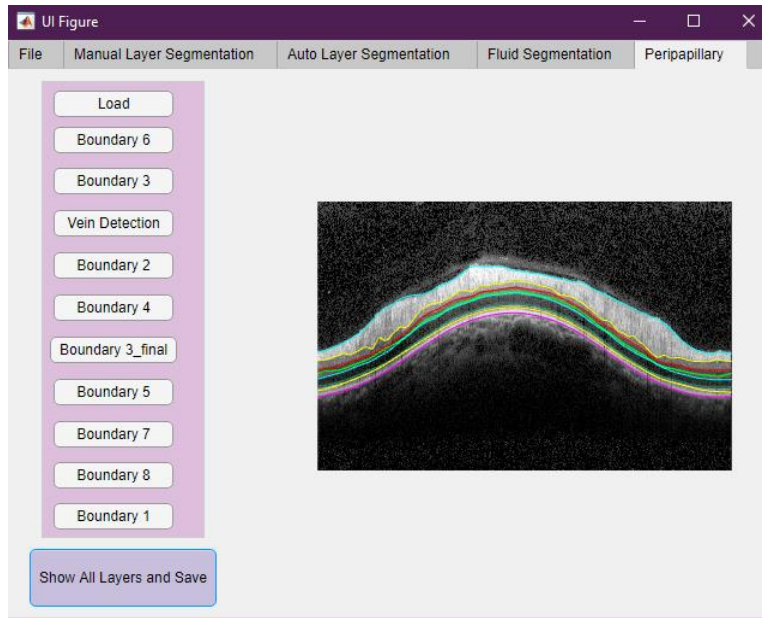


Fig. 19. Peripapillary tab

2.6. Functions Description

Table 4 brings a detailed description of all functions in the proposed Livelayer software.

Table 4. Main functions in the Livelayer software

Tab	Section in the Tab	Relevant Functions
File	.vol	Read_VOL_func
	.octbin	readbin
Manual Layer Segmentation	Boundaries	Free_hand
Auto Layer Segmentation	Semi-Automatic	lwcontour , resize_contour
	Manual-Grid	ginputc , resize_contour
	Layer Correction	manual_correction
Fluid Segmentation	Semi-Automatic	lwcontour
	Manual	MATLAB imfreehand
Peripapillary	Boundaries	lwcontour , resize_contour
		find_vein
		alignment

3. Illustrative Example

Fig. 20 is brought to visualize an overview of the software for the reader. While each tab could be utilized independently from others, results can be merged together and compared for research purposes.

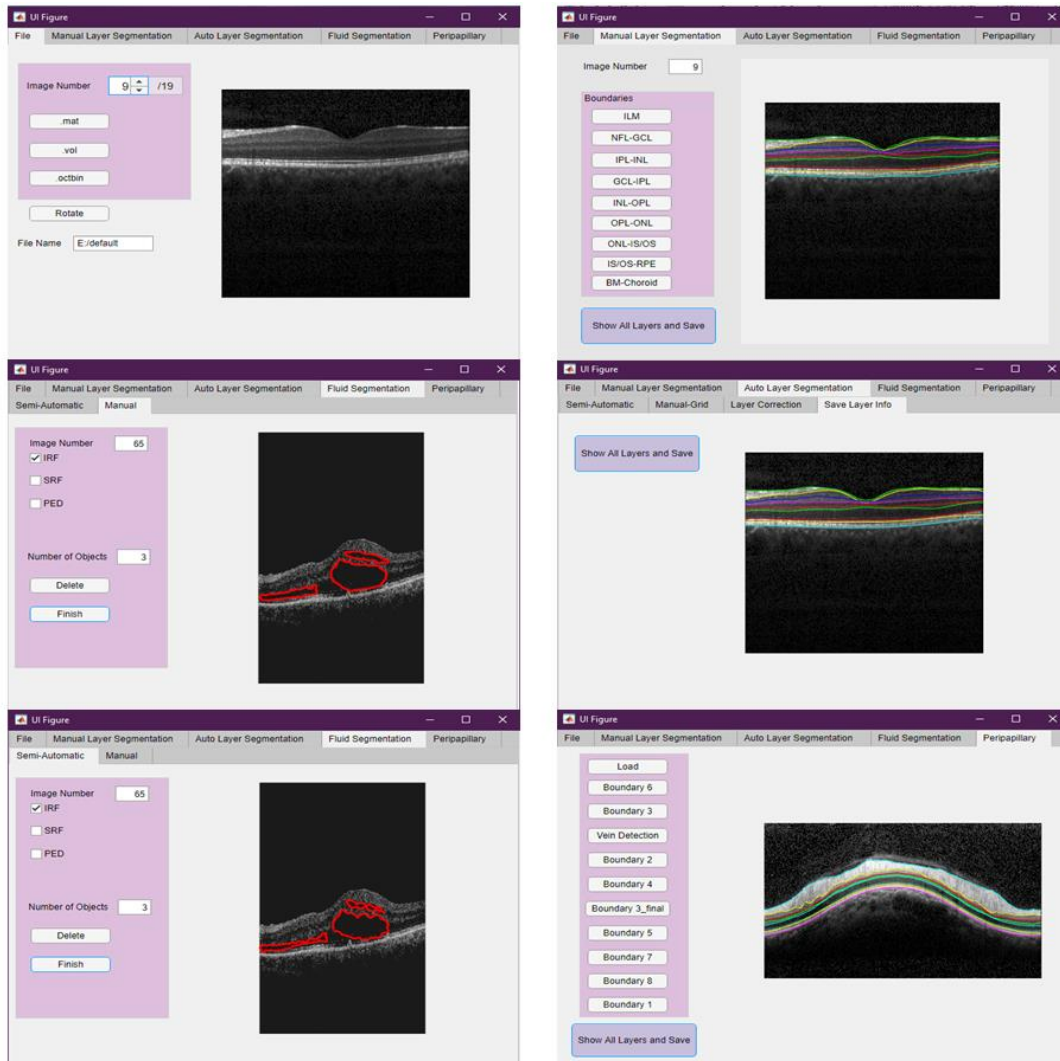


Fig. 20. A review of the primary tabs in the Livelayer software.

4. Impact

Our software is principally devised to benefit ophthalmologists and researchers by reducing the dedicated time to OCT layer segmentation as well as providing a straightforward, easy to manipulate environment for them. Its structure design makes it be quickly learned and conveniently used without facing any problem. Lack of an appropriate user interface for OCT layer and fluid segmentation raised

our enthusiasm to work on this paper and we tried to fully clarify every helpful point which might be critical to running this software for the readers. Before writing this paper, we assessed practical aspects of our software by distributing it among some biomedical engineering graduate students and two ophthalmologists whose satisfaction with its time saving, multifunctional and costless features motivated us to improve our job through handing out the software to larger communities.

5. Conclusions

According to a thorough evaluation of our semi-automatic devised algorithm, we deduced that the method is feasible to be employed on real and artificial data, significantly reduces the amount of time layers and fluids need to be segmented and also allows researchers to combine it with their own codes in order to achieve the best result. On account of being an open-source product, it can be upgraded to newer versions by either adding more essential tabs to it or by improving current tabs and algorithms so that they can be applied more efficiently.

Conflict of interest

Acknowledgments

References

1. Podoleanu, A.G., *Optical coherence tomography*. The British journal of radiology, 2005. **78**(935): p. 976-988.
2. Hajizadeh, F. and R. Kafieh, *Introduction to Optical Coherence Tomography*, in *Atlas of Ocular Optical Coherence Tomography*. 2018, Springer. p. 1-25.
3. Schneider, E., et al., *Optical coherence tomography reveals distinct patterns of retinal damage in neuromyelitis optica and multiple sclerosis*. PloS one, 2013. **8**(6).

4. Hee, M.R., et al., *Optical coherence tomography of the human retina*. Archives of ophthalmology, 1995. **113**(3): p. 325-332.
5. Wu, M., et al., *Automatic subretinal fluid segmentation of retinal SD-OCT images with neurosensory retinal detachment guided by enface fundus imaging*. IEEE Transactions on Biomedical Engineering, 2017. **65**(1): p. 87-95.
6. MathWorks, "MATLAB version R2018a", N. ed: The Mathworks Mathworks, Editor. 2018.
7. Huang, Y., et al., *Development of a semi-automatic segmentation method for retinal OCT images tested in patients with diabetic macular edema*. PloS one, 2013. **8**(12).
8. Sonoda, S., et al., *Kago-Eye2 software for semi-automated segmentation of subfoveal choroid of optical coherence tomographic images*. Japanese journal of ophthalmology, 2019. **63**(1): p. 82-89.
9. Zhao, L., et al., *Semi-automatic OCT segmentation of nine retinal layers*. Investigative Ophthalmology & Visual Science, 2012. **53**(14): p. 4092-4092.
10. Liu, X., et al., *Semi-supervised automatic segmentation of layer and fluid region in retinal optical coherence tomography images using adversarial learning*. IEEE Access, 2018. **7**: p. 3046-3061.
11. Motamedi, S., et al., *Normative data and minimally detectable change for inner retinal layer thicknesses using a semi-automated OCT image segmentation pipeline*. Frontiers in Neurology, 2019. **10**: p. 1117.
12. Dijkstra, E.W., *A note on two problems in connexion with graphs*. Numerische mathematik, 1959. **1**(1): p. 269-271.
13. Chodorowski, A., et al. *Color lesion boundary detection using live wire*. in *Medical Imaging 2005: Image Processing*. 2005. International Society for Optics and Photonics.
14. Canny, J., *A computational approach to edge detection*. IEEE Transactions on pattern analysis and machine intelligence, 1986(6): p. 679-698.
15. Sobel, I., *History and definition of the sobel operator*. Retrieved from the World Wide Web, 2014. **1505**.
16. Sobel, I. and G. Feldman, *A 3x3 isotropic gradient operator for image processing*. a talk at the Stanford Artificial Project in, 1968: p. 271-272.
17. Serra, J., *Image analysis and mathematical morphology*. 1983: Academic Press, Inc.
18. Matheron, G. and J. Serra. *The birth of mathematical morphology*. in *Proc. 6th Intl. Symp. Mathematical Morphology*. 2002. Sydney, Australia.
19. Tso, M.O., *Pathology of cystoid macular edema*. Ophthalmology, 1982. **89**(8): p. 902-915.
20. Xu, X., et al., *Stratified sampling voxel classification for segmentation of intraretinal and subretinal fluid in longitudinal clinical OCT data*. IEEE transactions on medical imaging, 2015. **34**(7): p. 1616-1623.
21. Gonzalez, A. and G. Khurshid, *Treatment of retinal pigment epithelial detachment secondary to exudative age-related macular degeneration*. American journal of ophthalmology case reports, 2018. **9**: p. 18-22.